Two-photon magnetospectroscopy of A-exciton states in CdS

D. G. Seiler
Francis Bitter National Magnet Laboratory, Massachusetts Institute of Technology, Cambridge, Massachusetts 02139
and Department of Physics, North Texas State University, Denton, Texas 76203

D. Heiman
Francis Bitter National Magnet Laboratory, Massachusetts Institute of Technology, Cambridge, Massachusetts 02139

R. Feigenblatt
Francis Bitter National Magnet Laboratory, Massachusetts Institute of Technology, Cambridge, Massachusetts 02139
and Department of Electrical Engineering, Massachusetts Institute of Technology, Cambridge, Massachusetts 02139

R. L. Aggarwal and B. Lax
Francis Bitter National Magnet Laboratory, Massachusetts Institute of Technology, Cambridge, Massachusetts 02139
and Department of Physics, Massachusetts Insititute of Technology, Cambridge, Massachusetts 02139
(Received 22 December 1981)

High-resolution spectra are obtained for the free A excitons in CdS by two-photon absorption using photoconductivity techniques. At zero applied magnetic field the anisotropy splitting of the $2P$ and $3P$ exciton states is observed and interpreted with an anisotropic effective-mass Hamiltonian. The energies of these states are measured as a function of magnetic field up to $B \simeq 10$ T. The magnetic field dependences are analyzed in terms of linear Zeeman splitting and diamagnetic interactions. At low fields the diamagnetic contribution gives the usual quadratic field dependence but deviates significantly at higher fields. At a given field, the deviation is found to increase dramatically with increasing quantum number n. This deviation is fitted by variational calculations developed by Larsen, which take into account the interaction of states through the diamagnetic term in the Hamiltonian. The magnetic field dependence of these states allow us to determine the masses as $m_e^{\perp}=(0.210\pm0.003)m_0$ and $m_h^{\perp}=(0.64\pm0.2)m_0$. At $B=0$ the narrow laser linewidths (0.05 meV) allow an accurate determination of the A-exciton binding energy of 27.4 ± 0.8 meV and the anisotropy parameter of 0.797 ± 0.013 from which the energy gap $E_g^A=2582.5\pm0.2$ meV at $T=1.8$ K is calculated. Finally, the temperature dependence of the A gap is determined.

I. INTRODUCTION

Excited states ($n \geq 2$) of the free exciton in CdS have been studied previously by linear absorption[1-3] and two-photon absorption (TPA).[4-8] Magnetic field effects on these excitons were studied up to $B=3$ T by Hopfield and Thomas[1] in high resolution and up to $B=10$ T by Shah and Daman[2] with moderate resolution using one-photon techniques. Daman *et al.*[7] studied $2P$ exciton states by two-photon magnetoabsorption (TPMA) techniques for a magnetic field of 5 T parallel to the hexagonal c axis. Through polarization studies they were able to understand the Zeeman splitting of the $2P_{\pm1}$ states and fine structure splitting of the $2P_{+1}$, $2P_{-1}$, and $2P_z$ states. We present here the results of high-resolution, TPA magneto-optical experiments on the free-exciton excited states in CdS up to $B \simeq 10$ T. Both Zeeman splitting and diamagnetic shifts of the $n=2$ and $n=3$ exciton states are investigated. At these fields the higher-lying exciton states show considerable deviation from quadratic diamagnetic behavior. This deviation is explained by considering level interactions or state mixing using variational calculations due to Larsen.[9] The high reso-

lution obtained in the present experiment enables us to determine some material parameters of CdS more accurately than in previous studies.

CdS has a hexagonal wurtzite structure.[10] This structural anisotropy causes crystal-field splitting, which interacts with the spin-orbit coupling to split the valence band into three bands, A, B, C, each twofold degenerate with spin considered. The lowest band gap is due to the A-valence band and is at the Brillouin-zone center at $E_g^A \simeq 2.582$ eV. The conduction band with electron mass $m_e \simeq 0.2 m_0$ produces free excitons associated with each valence band having an effective Rydberg of $\simeq 27$ meV and a ground-state radius of $\simeq 30$ Å. The pioneering work of Hopfield and Thomas[1] utilized a magnetic field to study these excitons using one-photon absorption. They determined values for the exciton binding energy, electron and hole masses, the electron and hole spin g factors and analyzed the Zeeman splitting and diamagnetic shifts up to $B = 3$ T. At these fields the magnetic perturbation on the wave functions is weak in comparison to the Coulomb interaction, while at higher magnetic fields the Lorentz force on the exciton becomes comparable to the Coulomb force. As a result, the wave functions contract to such an extent that deviations from quadratic diamagnetic behavior occur. The magnetic field causes mixing of the $B = 0$ wave functions through the ordinary diamagnetic perturbation. This interaction is known to couple states having $\Delta l = 0, \pm 2$ and $\Delta m_l = 0$ for all principal quantum numbers ($\Delta n \neq 0$ or $\Delta n = 0$). Higher-lying energy levels tend to repel lower states down in energy. This effect reduces the quadratic dependence of the levels and eventually causes it to once again approach a linearlike dependence. This departure from the low-field behavior is expected to occur at lower fields for excited-state excitons. This occurs because the wave functions are much larger and hence have a smaller Coulomb interaction to overcome. Thus, we expect to see $n = 3$ exciton states deviate much more from a quadratic dependence than $n = 2$ states at a given field.

The energy-level spectra of the free excitons are produced in the present study by two-photon absorption. In this particular experiment two photons are simultaneously absorbed, where one is fixed in energy and the other is tunable and their sum is made equal to the exciton level. Since both photon energies are below the gap, the absorption occurs throughout the bulk of the sample, which places less importance on the sample surface. The absorption is monitored by the photoconductivity of the samples and the spectral resolution is determined by the linewidth of the laser which is less than 0.05 meV. To our knowledge this is the first time that the photoconductivity technique has been used to obtain the TPA spectra of free excitons in semiconductors.

II. EXPERIMENTAL WORK

The single-crystal samples of CdS were high-purity platelets of 10^{-3}-cm thickness grown from the vapor phase. The crystals used were all in the as-grown condition. Overall sizes were approximately 1×5 mm^2 with the hexagonal c axis lying in the platelet plane parallel to the longest side. Indium electrodes were attached to the surface by melting pure indium onto the samples at 410 °C while in a nitrogen environment. 6-μm-thick indium-gold ribbon was used for the contact wires. Patterns obtained on a Tektronix I-V curve tracer at both very low and very high voltages were symmetric, indicating good Ohmic contacts. To minimize any possible external strain on the crystals, the samples themselves were not epoxied or glued directly to any base. Instead, all samples were placed on polished sapphire substrates and only the flexible ribbon wire was carefully glued to the sapphire. Typical room-temperature resistivities of "good" crystals were $\simeq 10^3$ Ω cm in the light, while dark resistivities were $\geq 10^6$ Ω cm. [Good crystals showed clear resolution of the $A(2P_0)$ line from the $A(2P_{\pm 1})$ line at $B = 0$ with full width at half-maximum (FWHM) linewidths $\simeq 0.3$ meV.] We expect that $N_d - N_a < 10^{16}$ cm^{-3}, indicating some degree of compensation. Voltages up to 45 V were applied across the sample ($E \lesssim 100$ V/cm) without affecting the spectra. Of the half-dozen samples tried only one half showed the narrow $B = 0$ spectral linewidths; the others had $A(2P)$ linewidths approximately twice as wide.

The spectrum of the exciton states was taken by observing the increase in light absorption as monitored by the increase in sample conductivity as a function of photon energy. This method has been used previously by Button *et al.*[11] and more recently by Seiler *et al.*[12] in studying two-photon-induced photoconductivity in InSb using CO_2 lasers. Photoconductive structure using one-photon spectroscopy has been observed at the positions of the free excitons.[13] The exact mechanism causing breakup of the excitons into free electrons and holes is a

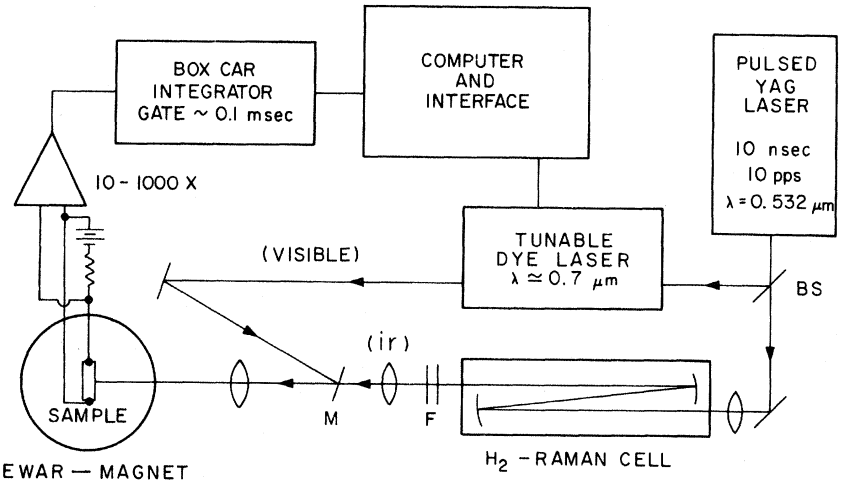

FIG. 1. Schematic diagram of two-photon magnetoabsorption spectroscopy equipment. The doubled-YAG laser output is divided by a beam splitter (BS) in order to pump a tunable dye laser and triple-pass stimulated-Raman-shifting cell. The unwanted Stokes and anti-Stokes outputs of the cell are attenuated by filters (F). The infrared and visible beams are combined by a dielectric mirror (M). The absorption as a function of total photon energy was monitored by measuring the photoinduced conductivity change.

matter of conjecture; presumably it occurs through interaction with defect or impurity centers.[14]

A Q-switched yttrium aluminum garnet (YAG) laser was used to produce two light beams as seen in Fig. 1, one tunable at $\hbar\omega_v \simeq 1.8$ eV from a dye laser and the other fixed at $\hbar\omega_{ir}=0.7840$ eV produced by stimulated Raman scattering.[15] The YAG second harmonic at $\lambda=0.532$ μm was divided by a beam splitter in order to simultaneously pump the tunable dye laser using LD688 dye and a Raman-shifting cell. The 50-cm-long cell contained hydrogen gas at 450 psi. The pump beam was focused three times inside the cell by initially using a 50-cm focal-length lens placed outside the cell and two concave mirrors (25-cm radius of curvature) mounted inside the cell. Triple passing the cell allowed lower threshold power, approximately one half that obtainable with a single pass. The third-Stokes-shifted ir light was selected by blocking the unwanted Stokes and anti-Stokes light by a long pass filter (0.57 μm) and a 1-mm-thick silicon window. After the visible and ir beams were made to overlap in time they were combined collinearly using a dielectric mirror that reflected the red light while transmitting the ir. The beams were then focused onto the sample using a 30-cm focal-length spherical lens. The peak power of the ir beam was about 5 kW while the visible beam was the order of 10—100 W. The sample was mounted in a variable temperature Dewar containing pumped liquid He at 1.8 K or flowing He gas for higher temperatures. The optical Dewar tail was mounted in a 2-in. bore Bitter magnet solenoid having radial access to the light in a Voigt configuration. The applied current, c axis, and B field were all parallel. A 10-MΩ resistor in series with a battery was placed across the sample. The photoinduced voltage change across the sample was extracted by a low-pass—high-pass filter combination, then amplified between 10 and 1000 times. This output was sampled by a boxcar integrator of gatewidth 0.1 msec. The spectral scans were taken via a computer that read the boxcar output with an analog-to-digital converter while scanning the tunable dye laser through a stepping-motor-shaft-encoder combination. Fluctuations in the photoconductivity signal at 60 Hz were eliminated by locking the laser pulses to a subharmonic of the 60-Hz line frequency.

Spectra were also taken in a single-beam experimental configuration, where $\hbar\omega_{ir}$ was one half the exciton energy. With additional pump power, the dye laser output could be directed into the Raman cell producing "tunable," near-infrared light. The single-beam setup was found to give spectra without the flat background present in the two-beam spectra. Also alignment was much easier since the overlap of two beams is not necessary.

III. THEORY

A. Free-exciton energy levels

The energy-level spectrum of the free excitons in CdS can be conveniently calculated within the

effective-mass approximation. The basic Hamiltonian appropriate to this anisotropic situation has been derived in detail by several authors using slightly different parameter notations suitable for perturbation or variational solutions. Using a center-of-mass coordinate system where the center-of-mass motion is set equal to zero, the effective one-particle Schrödinger equation for an electron-hole pair interacting with each other by the Coulomb field in a wurtzite-type material such as CdS can be written as[16]

$$\left[\frac{-\hbar^2}{2\mu_\perp}\left(\frac{\partial^2}{\partial x^2}+\frac{\partial^2}{\partial y^2}\right)-\frac{\hbar^2}{2\mu_{||}}\frac{\partial^2}{\partial z^2}-\frac{e^2}{\{K_\perp K_{||}[x^2+y^2+(K_\perp/K_{||})z^2]\}^{1/2}}\right]F(\vec{r})=EF(\vec{r})\ . \tag{1}$$

Here z is parallel to the c axis, $F(\vec{r})$ is the exciton envelope function, $E=E_{ex}-E_g$, $K_\perp$ and $K_{||}$ are components of the dielectric tensor, and $\mu_\perp$ and $\mu_{||}$ are components of the effective reduced-mass tensor of the exciton, i.e.,

$$\frac{1}{\mu_\perp}=\frac{1}{m_e^\perp}+\frac{1}{m_h^\perp},\quad \frac{1}{\mu_{||}}=\frac{1}{m_e^{||}}+\frac{1}{m_h^{||}}\ . \tag{2}$$

Making the substitution

$$x'=x,\quad y'=y,\quad z'=\frac{K_\perp}{K_{||}}z\ ,$$

Eq. (1) becomes

$$\left[-\frac{\hbar^2}{2\mu_\perp}\left(\frac{\partial^2}{\partial x'^2}+\frac{\partial^2}{\partial y'^2}\right)-\frac{\hbar^2}{2\mu_{||}}\frac{K_\perp}{K_{||}}\frac{\partial^2}{\partial z'^2}-\frac{e^2}{K(x'^2+y'^2+z'^2)^{1/2}}\right]F(\vec{r}')=EF(\vec{r}')\ . \tag{3}$$

It is convenient to write Eq. (3) in the dimensionless form

$$\left[-\left(\frac{\partial^2}{\partial x^2}+\frac{\partial^2}{\partial y^2}+\frac{\partial^2}{\partial z^2}\right)-\frac{2}{r}\right]F(\vec{r})=EF(\vec{r})\ , \tag{4}$$

where we have dropped the primes, and the units of length and energy are given by

$$a_B=\frac{\hbar^2K}{\mu_\perp e^2},\quad \mathscr{R}^*=\frac{\mu_\perp e^4}{2\hbar^2K^2}\ , \tag{5}$$

and are, respectively, the reduced Bohr radius and the effective Rydberg binding energy. The anisotropy parameter $\gamma=(\mu_\perp K_\perp)/(\mu_{||}K_{||})$. This same equation was given by Faulkner for solving the donor impurity-level case in silicon and germanium at zero magnetic field.[17]

In the presence of a uniform external magnetic field parallel to the c axis and using a cylindrical gauge where the vector potential $\vec{A}=(\vec{B}\times\vec{r})/2$ results in the addition of several terms to the one-particle Hamiltonian of Eq. (3):

$$\frac{m_h^\perp-m_e^\perp}{m_h^\perp+m_e^\perp}\eta L_z+\eta^2(x^2+y^2)/4+g_zS_z\eta/2\ , \tag{6}$$

where $\eta=\mu_B^*B/\mathscr{R}^*$ is a dimensionless measure of the strength of the magnetic field B, the effective Bohr magneton $\mu_B=e\hbar/2\mu_\perp c$, L_z is the z component of the orbital angular momentum operator, g_z is the parallel component of the exciton g factor, and S_z is the z component of the exciton spin angular momentum. The first term linear in B is due to the ordinary Zeeman effect arising from the $\vec{A}\cdot\vec{P}$ terms for the electron and hole, while the last term, also linear in B, is due to the interaction of the electron and hole spins with the magnetic field. The middle term represents the diamagnetic effect arising from the A^2 term which is usually considered to be quadratic in B; at high enough magnetic fields and/or for higher excited exciton states considerable deviation from a quadratic behavior can be expected as a result of the strong mixing of states of different principle quantum number.

In order to calculate the eigenvalues of the Hamiltonian in Eq. (4) for the $2P$ levels at $B=0$ and the diamagnetic part of the Hamiltonian in Eq. (6) we employ the following variational trial functions[9]:

$$\psi_{2P_\pm}=\rho e^{-A_1\rho^2-A_2\tilde{r}}\ ,$$

$$\psi_{2P_0}=ze^{-A_1\rho^2-A_2\tilde{r}}\ ,$$

TABLE I. Calculated energy levels of the A excitons in CdS. Variational calculations of the binding energy, in units of $\mathscr{R}^*$, are compared with those of Faulkner (Ref. 17) and Praddaude (Ref. 19). $B=0$ at $\eta=0$ and $B\simeq 7.5$ T at $\eta=0.1$.

Anisotropic model	$\eta=0$ $[\gamma^{1/3}=(0.729)^{1/3}=0.900]$		$\eta=0.1$ Spherical model ($\gamma=1$)	
Energy level	This paper	Faulkner	This paper	Praddaude
$2P_0$	0.3010	0.3009	0.3239	0.3248
$2P_-$	0.2656	0.2656	0.3995	0.4017
$3P_0$	0.1342	0.1342	0.1381	0.1398
$3P_-$	0.1183	0.1184	0.1583	0.1624

where $\tilde{r}=(\rho^2+\alpha z^2+\beta^2)^{1/2}$, $\rho^2=x^2+y^2$. The variational parameters[9] A_1, A_2, α, and β are optimized for each state and magnetic field of interest by minimizing

$$\langle\psi_{2P}\,|\,H\,|\,\psi_{2P}\rangle/\langle\psi_{2P}\,|\,\psi_{2P}\rangle\ .$$

The $3P$ eigenvalues are computed by using the trial functions[18]

$$\psi_{3P_\pm}=\rho(2-\xi\tilde{\tilde{r}})e^{-D\rho^2-E(\rho^2+\xi z^2)^{1/2}}+C_\pm\psi_{2P_\pm}\ ,$$

$$\psi_{3P_0}=z(2-\xi\tilde{\tilde{r}})e^{-D\rho^2-E(\rho^2+\xi z^2)^{1/2}}+C_0\psi_{2P_0}\ ,$$

where $\tilde{\tilde{r}}=(\rho^2+\delta z^2+\theta^2)^{1/2}$. The variational parameters D, E, ξ, δ, and θ are optimized in a fashion similar to the $2P$ case. The C parameters were determined by forcing orthogonality between $3P_\pm$ and $2P_\pm$, and between $3P_0$ and $2P_0$ for each choice of the other parameters.

The accuracy of these $2P$ and $3P$ variational calculations can be seen from the results given in Table I for both $\eta=0$ and $\eta=0.1$. At zero field we compare our results with those of Faulkner[17] who used the Rayleigh-Ritz approach to determine the values of $\mathscr{R}^*$ for certain values of γ. Using a value of $\gamma=0.729$ which corresponds to his tabulated $\gamma^{1/3}=0.900$ gives excellent agreement for the various energy levels shown in Table I. Solutions in a magnetic field ($\gamma=0.1$) are compared to the more accurate spherical results of Praddaude[19] obtained by expansion of the wave function in Laguerre polynomials for hydrogenlike atoms in a magnetic field. Our calculated binding energies, in units of $\mathscr{R}^*$, are lower than Praddaude's by 0.0009, 0.0022, 0.0017, and 0.0041 for the $2P_0$, $2P_-$, $3P_0$, and $3P_-$ states, respectively. This is to be expected from a variational calculation. However, the relative spacings of the energy levels $E(2P_\pm)-E(2P_0)$, $E(3P_0)-E(2P_0)$, and $E(3P_\pm)-E(2P_0)$ levels are generally in closer agreement: Praddaude's, $+0.0769$, -0.1850, -0.1624; our results, $+0.0756$, -0.1858, and -0.1656, respectively. As we shall see later, these errors are approximately the same as the uncertainties in field-dependent energy shifts of each of the respective levels. Consequently, we expect our variational calculations to adequately explain the data.

B. Two-photon absorption

The basic theory of two-photon processes was formulated by Göppert-Mayer in 1931.[20] Using second-order perturbation theory and making the dipole approximation gives the probability per unit time per unit volume $W^{(2)}(E)$ that the system makes a transition from an initial state i to a final state f of energy $E=\hbar(\omega_1+\omega_2)$ above the ground state, while the field loses one quantum each of energy $\hbar\omega_1$ and $\hbar\omega_2$.[21] Thus,

$$W^{(2)}(E)=\frac{2\pi}{\hbar}\left[\frac{eA_{01}}{mc}\right]^2\left[\frac{eA_{02}}{mc}\right]^2|A_{fi}^{(2)}|^2\times\delta(E_f-E_i-\hbar\omega_1-\hbar\omega_2)\ , \tag{7}$$

where A_{01} and A_{02} are the magnitude of the vector potentials of the radiation beams polarized in the fixed directions $\hat{\epsilon}_1$ and $\hat{\epsilon}_2$, and $A_{fi}^{(2)}$ is the composite matrix element given by

$$A_{fi}^{(2)}=\sum_I\left[\frac{(\vec{\mathrm{P}}_{fI}\cdot\hat{\epsilon}_1)(\vec{\mathrm{P}}_{Ii}\cdot\hat{\epsilon}_2)}{E_I-E_i-\hbar\omega_2}+\frac{(\vec{\mathrm{P}}_{fI}\cdot\hat{\epsilon}_2)(\vec{\mathrm{P}}_{Ii}\cdot\hat{\epsilon}_1)}{E_I-E_i-\hbar\omega_1}\right]. \tag{8}$$

Here P_{fi} and P_{Ii} are matrix elements of the dipole operator and the sum is over all possible intermediate states I. The quantity usually measured in a TPA experiment is β which is related to the transition rate per unit volume by the expression

$$\beta=(\hbar\omega_1+\hbar\omega_2)\frac{W^{(2)}(E)}{I_1 I_2} .$$

A knowledge of the laser beam properties both in space and time is needed to determine β and a lack of complete beam characterization can lead to large uncertainties. As pointed out by Bechtel and Smith,[22] the absorption may depend upon the laser pulsewidth because absorption by two-photon-created excess carriers is not negligible.

For the purposes of this study we are interested in the two-photon resonance condition given in the δ function of Eq. (7). Thus whenever $E_f-E_i=\hbar\omega_1+\hbar\omega_2$ we expect to observe a maximum in the two-photon absorption and hence the greatest photoconductive response. The complications just mentioned should not affect this resonance condition.

The transition probabilities depend upon the light polarization as seen in Eq. (8). There have been several calculations and tabulations of the form of these angular dependences in order that they might be readily available for the analysis of experimental data. Inoue and Toyozawa[23] gave the angular dependence of two-photon transitions in which either the initial or final state transforms according to the totally symmetric representation of the point group. This work was subsequently extended by Bader and Gold[24] to (1) the allowed transitions between states belonging to all irreducible representations of the point group and (2) the double-group representations encountered when spin-orbit coupling is included. Both Stafford and Sondergeld[6] and Nguyen *et al.*[4] found no evidence for TPA to final S-exciton states, in contrast to the work of Pradere and Mysyrowicz.[5] The polarization dependence of these matrix elements was used by Nguyen *et al.* to show that the $1S$-exciton ground state is an effective intermediate state when one photon from a dye laser is nearly resonant with the $1S$ exciton energy, while the other photon is produced by a CO_2 laser.

The allowed TPA selection rules at the Γ point can be determined from group theory applied to the C_{6V} symmetry of CdS-type crystals. The symmetries of the A excitons are then a result of the Γ_7 conduction band and Γ_9 valence-band symmetries along with the symmetries of the hydrogenic states of the exciton in the center-of-mass coordinate system. We summarize the results in Table II where various exciton states, their decomposition into various symmetries, and the allowed one- and two-photon transitions are given. For $\vec{E}||c$, the dipole radiation representation is Γ_1 and for $\vec{E}\perp c$, it is Γ_5. A magnetic field parallel to the hexagonal axis of the crystal represents a perturbation of symmetry Γ_2. Group theory can then be used to calculate g values for all the exciton states as shown in Table II.

IV. RESULTS AND CONCLUSIONS

The TPA spectra near the A exciton region are shown in Fig. 2. The lowest observable exciton states are the $2P$ levels. Even though a Γ_6 $1S$ or $2S$ transition is allowed in TPA, no evidence for their existence was found. These observations were first made by Stafford and Sondergeld[6] and later by Nguyen *et al.*[4] using TPA. Evidently the oscillator strength for this Γ_6 state is very small. At

TABLE II. CdS exciton states and their symmetries. The allowed one- and two-photon transitions and their polarizations are shown for $\vec{E}\perp c$ ($\perp$) and $\vec{E}||c$ ($||$). The corresponding g values for $\vec{B}||c$ are also given.

State	Possible symmetries	One-photon allowed	Two-photon allowed	g values
$1S,2S$	Γ_5,Γ_6	$\Gamma_5(\perp)$		$\lvert g_{e\|\|}-g_{h\|\|}\rvert$
			$\Gamma_6(\perp,\perp)$	$\lvert g_{e\|\|}+g_{h\|\|}\rvert$
$2P_0$	Γ_5,Γ_6	$\Gamma_5(\perp)$		$\lvert g_{e\|\|}-g_{h\|\|}\rvert$
			$\Gamma_6(\perp,\perp)$	$\lvert g_{e\|\|}+g_{h\|\|}\rvert$
$2P_{\pm1}$	$\Gamma_1,\Gamma_2,\Gamma_3,\Gamma_4,\Gamma_5,\Gamma_6$	$\Gamma_5(\perp)$		$\lvert 2g_{\mu\|\|}-g_{e\|\|}-g_{h\|\|}\rvert$
		$\Gamma_1,\Gamma_2(\|\|)$		$\lvert 2g_{\mu\|\|}+g_{e\|\|}-g_{h\|\|}\rvert$
			$\Gamma_1,\Gamma_2(\perp,\perp$ or $\|\|,\|\|)$	$\lvert 2g_{\mu\|\|}+g_{e\|\|}-g_{h\|\|}\rvert$
			$\Gamma_6(\perp,\perp)$	$\lvert 2g_{\mu\|\|}-g_{e\|\|}+g_{h\|\|}\rvert$

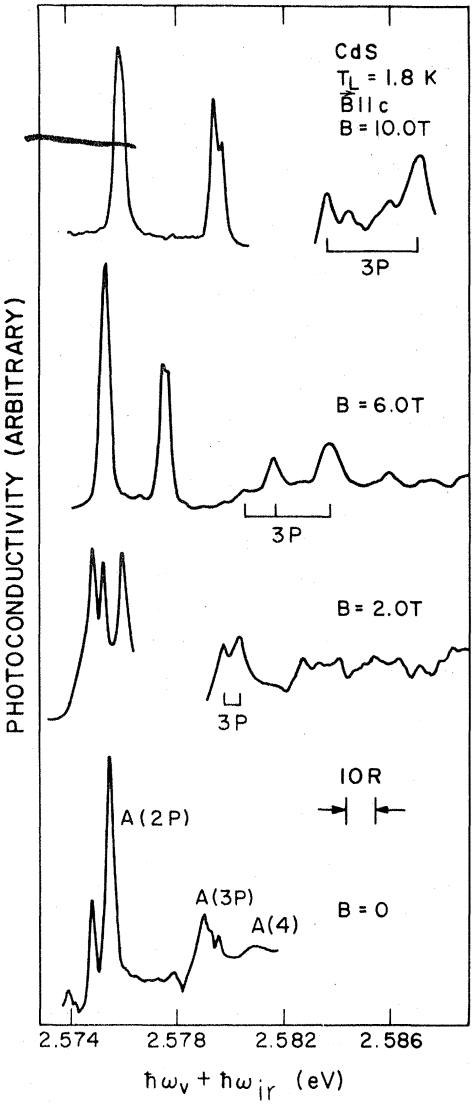

FIG. 2. Photoconductivity vs total photon energy $\hbar\omega_v + \hbar\omega_{ir}$ near the A-exciton region in CdS platelets for various magnetic fields. The magnetic field was parallel to the hexagonal c axis in a Voigt configuration with $\vec{E}$ perpendicular to c for the two photons at a lattice temperature of $T_L = 1.8$ K. The instrumental resolution $R = 0.1$ meV is narrower than the intrinsic linewidths.

$B = 0$ the $2P$ states clearly show the expected anisotropy splitting corresponding to $2P_0$ ($m_l = 0$) and $2P_\pm$ ($m_l = \pm 1$). The $2P$ structure has allowed contributions from both the Γ_1, Γ_2 and the Γ_6 symmetry states which lie close in energy so that one cannot resolve them at $B = 0$. At $B = 10$ T, there is fine-structure splitting observable in the $2P_+$ state which is caused by the slightly different g factors for the $\Gamma_1 + \Gamma_2$ and the Γ_6 states. Similar splitting at $B = 0$ has been seen by Hopfield and Thomas[1] and Nguyen *et al.*[4] For the $3P$ states the signal-to-noise ratio at $B = 0$ was lower, resulting in poor resolution. In order to extract the peak positions many scans were taken on several samples. Zero-field results of the $3P_0$ and $3P_\pm$ states reported here are averages of these scans. This is the first experiment with enough resolution to resolve this anisotropy splitting of the $3P$ states. Zero-field positions of the observed A-exciton states in CdS are given in Table III where a comparison is also given with the one-photon results of Hopfield and Thomas[1] and Litton *et al.*[3] and the two-photon results of Stafford and Sondergeld[6] and Nguyen *et al.*[4] There is in general very good agreement.

The result of fitting our variational calculations to our data gives values for the effective Rydberg $\mathscr{R}^* = 27.4 \pm 0.8$ meV and the anisotropy parameter, $\gamma = 0.797 \pm 0.013$. Using our data and the less-accurate first-order perturbation approach of Hopfield and Thomas, whose state energies involve a mean Rydberg $\bar{\mathscr{R}}^*$ and a different anisotropy parameter γ', gives $\bar{\mathscr{R}}^* = 29.5$ meV and $\gamma' = 0.234$. This may be compared with Hopfield and Thomas's results of 28 ± 1 meV. Using $\mathscr{R}^* = 27.4$ meV and the energy levels for the anisotropic situation puts the energy gap for the A valence band at $E_g^A = 2582.5 \pm 0.2$ meV at $T = 1.8$ K. When a magnetic field is applied, the $n \geq 2$ peaks show both Zeeman splitting and diamagnetic shifting to higher energies. Although the $n = 3$ peaks shift to larger energy more rapidly, their splitting is seen to be nearly the same as for the $n = 2$ peaks. At higher fields, substructure in the $2P_\pm$ state and additional structure in the region of the $3P$ states are observed.

The energy positions of these peaks are plotted as a function of magnetic field in Fig. 3. The six states $2P_0$, $2P_\pm$, $3P_0$, and $3P_\pm$ are clearly observed with the exception of $2P_0$ and $2P_-$ at high fields, which appear to have merged together. This is the first time that the $3P$ states of CdS have been investigated in a magnetic field. An important result immediately apparent from Fig. 3 is that the $3P$-exciton states become linear in B at relatively low fields in agreement with the theoretical calculations of Praddaude.[19] Thus, the linear slopes of the exciton states become "Landau-like."[25,26]

The linear Zeeman splitting between P_+ and P_- pairs is shown in Fig. 4 for both the $n = 2$ and $n = 3$ states. The straight line is a best fit to the $2P_\pm$ states and results in $g_{\text{eff}}^{2P} = 6.39 \pm 0.08$, where the energy splitting is defined by $\Delta E \equiv g_{\text{eff}} \mu_B B$.

TABLE III. Experimental values of the zero-field A-exciton energies in CdS. All energies given in eV.

Energy level	Transition energy: One-photon results: Hopfield and Thomas (Ref. 1)	One-photon results: Litton *et al.* (Ref. 3)	Two-photon results: Stafford and Sondergeld (Ref. 6)	Two-photon results: Nguyen *et al.* (Ref. 4)	This paper
$1S\Gamma_6$	2.5524	2.5537			
$1S_L$	2.554 55	2.554 55			
$2S$		2.574 58			
$2P_0$	2.575 08			2.5754	2.574 64
		2.575 21	2.5745		
$2P_{\pm1}$	2.575 75			2.5762	2.575 33
$3S$		2.578 41			
$3P_0$					2.5789
		2.578 91		2.5815	
$3P_{\pm1}$					2.5793
$3D_{\pm2}$	2.579 77	2.579 23			
$n=4$	2.580 94	2.580 18			2.5809

The splitting of the $3P_{\pm}$ states gives the slightly smaller value of $g_{\text{eff}}^{3P}=6.09\pm0.20$. According to Table II the $2P_0\Gamma_6$ state should have a g factor of $|g_{e\|}+g_{h\|}|$. However, splitting of this line is not observed. If somehow the two-photon selection rule for this state allowed transitions to a Γ_5 symmetry level, then a g factor of $|g_{e\|}-g_{h\|}|$ would be predicted. Using $g_{e\|}=-1.78$ and $g_{h\|}=-1.15$ gives $g_{\text{eff}}=0.63$ which is small enough such that the splitting would not be observed at the low fields where the P_0 state is clearly resolved from the P_- state. We identify the observed fine-structure splitting of the $2P_+$ state with the $\Gamma_1+\Gamma_2$ and the Γ_6 states. Thus the average g value of these two lines from Table II is $g_{\text{eff}}=|2g\mu_{\|}|=|2(1/m_h^{\perp}-1/m_e^{\perp})|=6.39\pm0.08$. The energy difference of the fine-structure splitting of the $2P_+$ states is $(\frac{1}{2}|2g_{\mu\|}+g_{e\|}-g_{h\|}|-\frac{1}{2}|2g_{\mu\|}-g_{e\|}+g_{h\|}|)\mu_B B=|g_{e\|}-g_{h\|}|\mu_B B$. Thus at $B=10$ T, the observed splitting of 0.29 meV gives $|g_{e\|}-g_{h\|}|=0.50$. This compares favorably with the results of Venghaus *et al.*[27] of $|g_{e\|}-g_{h\|}|=0.56\pm0.05$, with $g_{e\|}=1.79\pm0.1$ and $g_{h\|}=1.23\pm0.1$ and the results of Damen *et al.*,[7] $|g_{e\|}-g_{g\|}|=0.55\pm0.05$.

In order to extract the quadratic diamagnetic contribution to the experimental energy shifts,

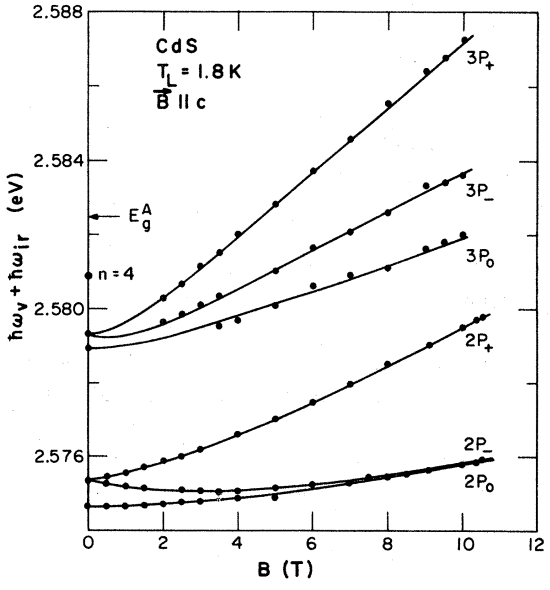

FIG. 3. Peak positions, in total photon energy $\hbar\omega_v+\hbar\omega_{ir}$, for the $2P$ and $3P$ A excitons in CdS platelets as a function of applied B field. The solid points were determined experimentally and the solid curves are theoretically obtained from variational calculations of the diamagnetic shifts along with use of the experimental g factors.

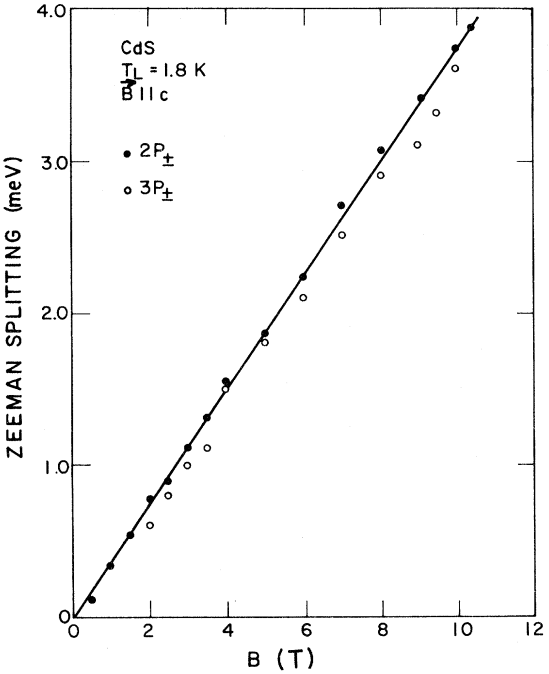

FIG. 4. Zeeman splitting of the $2P$ and $3P$ A excitons ($m_l = \pm 1$) in CdS as a function of magnetic field. The solid points represent the doublet splitting of the $2P_+$ and $2P_-$ pair, while the open circles are splittings of the $3P_+$ and $3P_-$ pair. The solid line is a linear fit to $2P$ with $g_{\text{eff}}(2P_\pm) = 6.39 \pm 0.08$.

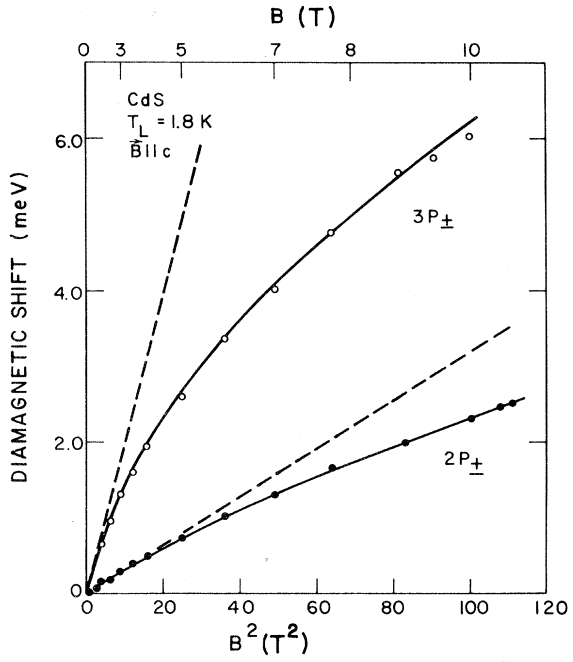

FIG. 5. Diamagnetic shift of the $2P_\pm$ and $3P_\pm$ A-exciton peaks in CdS as a function of applied B field squared. The solid points represent the $2P$ shift and the open circles are for $3P$. The diamagnetic shift is determined by subtracting one-half the Zeeman splitting from the total magnetic-field-induced shift. The lower dashed straight line is a fit to the $2P$ excitons at low fields. The solid curves are theoretical values determined from a variational calculation which includes level interactions. The upper dashed curve is a straight line with six times the slope of the lower dashed curve.

one-half of the Zeeman splitting is subtracted from the P_+ state and added to the P_- state. The results for both $2P_\pm$ and $3P_\pm$ are plotted as a function of B^2 in Fig. 5. The lower dashed curve is a straight-line fit to the experimental $2P_\pm$ points at low fields, $B < 3$ T. For $B > 3$ T the points deviate significantly; at $B = 10$ T the separation is 28%. The deviation from quadratic behavior of the $3P_\pm$ states is even much more pronounced. The slope at $B = 0$ gives the coefficient of the diamagnetic term from simple theory.[1] The upper dashed straight line near the $3P_\pm$ states has a slope 6 times that for the $2P_\pm$ as expected from this theory.

The diamagnetic shifts for the $2P$ and $3P$ states were calculated using the variational method described in the theory section. The solid lines in Fig. 5 show the results of these calculations. The fit is quite good. In Fig. 6 the diamagnetic shifts versus B are shown for all the exciton states. Excellent agreement is found between the experiment and theory. We note here that only *one* adjustable parameter $\mu_\perp$ was used to fit the field dependence of all six exciton states simultaneously. The best value was found to be $\mu_\perp = 0.158 \pm 0.002$, using $\mathcal{R}^* = 27.4$ meV and $\gamma = 0.797$, which were determined previously from the $B = 0$ energies. As a final test, the sum of the diamagnetic contribution from the theory and the experimentally determined Zeeman splitting is shown in Fig. 3 for all $2P$ and $3P$ states. Again, very good agreement is seen between the experimental points and the theory.

Using our experimentally determined values for $\mathcal{R}^*$ and $\mu_\perp$ in Eq. (2) gives a value of the mean dielectric constant $K = 8.9 \pm 0.2$. This and other material parameters are listed in Table IV along with values determined by other experiments.

Individual values for the electron and hole masses will now be extracted from our data in the most self-consistent manner. Two methods give results for both $m_e^\perp$ and $m_h^\perp$: (a) using our values for $\mu_\perp$ and $g_{\mu\|}$, and (b) using our values for $\mu_\perp$ and the exciton translational mass determined from resonant Brillouin scattering experiments.[28] These

TABLE IV. Material parameters for CdS. The values given are for low temperature ($T=1.8$ K) and for the A valence band.

Parameter	Definition	Present results	Other results	Reference	Comments
$\mathscr{R}^*$	$\frac{\mu_\perp e^4}{2\hbar^2 K^2}$	27.4±0.8 meV			from $B=0$ energies
			28±1	1	
γ	$\frac{(\mu_\perp K_\perp)}{(\mu_\parallel K_\parallel)}$	0.797±0.013			
	$\left[\frac{3-2\gamma'}{\gamma'+3}\right]$		0.793	1	from $\gamma'=0.222$ of Ref. 1
	in terms of anisotropy γ' in Ref. 1				
E_g^A		2.5825±0.0002 eV			
			2.582 eV	31	
$\mu_\perp$	$\left[\frac{1}{m_e^\perp}+\frac{1}{m_h^\perp}\right]^{-1}$	$(0.158\pm0.002)m_0$			from diamagnetic shifts and fit to variational calculations
			$(0.16)m_0$	1	
			$(0.16\pm0.03)m_0$	27	
$K=(K_\perp K_\parallel)^{1/2}$	$\frac{\mu_\perp e^4}{2\hbar^2\mathscr{R}^*}$	8.9±0.2			
			8.5	10	
			8.7	29	unpublished results of Barker and Summers mentioned in Ref. 29
$\lvert g_{e\parallel}-g_{h\parallel}\rvert$		0.50±0.15	0.62±0.06	1	
			0.56±0.05	27	
			0.55±0.05	7	
$\lvert 2g_{\mu_\parallel}\rvert$	$2\left\lvert\frac{1}{m_h^\perp}-\frac{1}{m_e^\perp}\right\rvert$	6.39±0.08			
			6.60	1	
$m_e^\perp$		$(0.210\pm0.003)m_0$			from $\mu_\perp$ and $g_{\mu_\parallel}$
			$(0.205\pm0.003)m_0$	28	from $\mu_\perp$ and exciton mass of $(0.89\pm0.1)m_0$ given in Ref. 28
			$(0.204\pm0.010)m_0$	1	
			$(0.190\pm0.002)m_0$	29	
$m_h^\perp$		$(0.64\pm0.02)m_0$			from $\mu_\perp$ and $g_{\mu_\parallel}$
			$(0.685\pm0.013)m_0$	28	from $\mu_\perp$ and exciton mass of $(0.89\pm0.01)m_0$ given in Ref. 28
			$(0.7\pm0.1)m_0$	1	

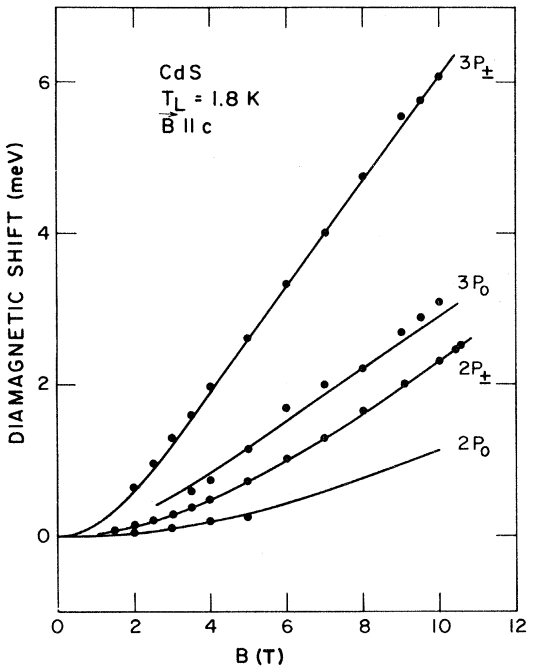

FIG. 6. Diamagnetic shift of the $2P$ and $3P$ A excitons in CdS as a function of applied B field. The experimental points for the P_0 states are the field-induced shifts, and the points for $P_\pm$ are obtained by taking the average of the P_+ and P_- field-induced shifts. The solid curves were determined from Larsen's variational calculations as described in the text. Only one adjustable parameter $\mu_\perp = (0.158 \pm 0.002) m_0$ was needed to simultaneously fit all curves.

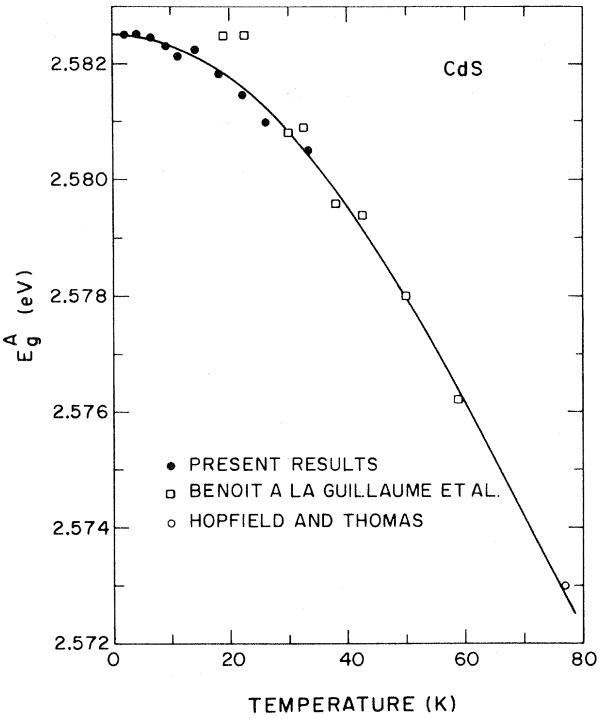

FIG. 7. Temperature dependence of the A energy gap in CdS. The solid points for E_g^A were derived from the positions of the $A(2P_\pm)$ exciton peaks by subtracting a constant binding energy (assuming a temperature-independent effective Rydberg). The open squares are from luminescence studies of Benoit à la Guillaume *et al.* (Ref. 30) and the open circle is from the reflectivity measurements of Thomas and Hopfield (Ref. 31).

results are tabulated in Table IV along with previously published results, including those of Henry and Nassau[29] for $m_e^\perp$.

The temperature dependence of the A gap is shown in Fig. 7. The low-temperature data points were determined from the energy of the $2P_\pm$ level at $B=0$ as a function of temperature. Above $T=35$ K the peak could not be observed above the noise level. Our data smoothly connects with results from luminescence by Benoit à la Guillaume *et al.*[30] and reflectivity by Thomas and Hopfield.[31]

In summary, we have shown that high-resolution two-photon-induced photoconductivity spectra are useful in studying absorption processes in semiconductors. The chief advantage of two-photon absorption is that it is a bulk process, and for strong absorption does not demand micrometer-thick samples or special attention to sample surfaces. The high resolution allows us to determine the anisotropy splitting of the $2P$ and $3P$ free-exciton states at zero magnetic field. These states show the expected linear Zeeman and quadratic diamagnetic dependence at low field. At higher fields the energy levels show a departure from the quadratic diamagnetism. This is especially striking for the higher quantum level $3P$ states. At these fields ($B \geq 2$ T) the $3P$ states show a linear field dependence similar to the Landau-level behavior. These effects are due to the mixing of states via the diamagnetic interaction. The magnitude of the deviation is fitted quite well by a variational method due to Larsen. Also, at the higher fields ($B \geq 6$ T) we see evidence of fine-structure splitting of the levels due to the small difference of the electron and hole spin g values. Finally, accurate values for the effective Rydberg and energy gap are determined by the zero-field exciton levels, as well as the effective electron and hole masses from the Zeeman splitting and diamagnetic interactions.

ACKNOWLEDGMENTS

We sincerely appreciate many useful conversations with D. M. Larsen, B. Wherrett, and H. C. Praddaude. D. M. Larsen is gratefully acknowledged for use of his computer programs for the variational calculations. We also thank D. Reynolds and C. Litton for supplying the excellent crystals and to D. Spears of Lincoln Laboratory for his help in making electrical contacts on the samples. The work of one of us (D.G.S.) was supported in part by the Office of Naval Research and NTSU and experimentally carried out of the Francis Bitter National Magnet Laboratory, which is supported by the National Science Foundation.

---

[1]J. J. Hopfield and D. G. Thomas, Phys. Rev. 122, 35 (1961).
[2]J. Shah and T. C. Damen, Solid State Commun. 9, 1285 (1971).
[3]C. W. Litton, D. C. Reynolds, and T. C. Collins, Phys. Rev. B 6, 2269 (1972).
[4]V. T. Nguyen, T. C. Damen, and E. Gornik, Appl. Phys. Lett. 30, 33 (1977).
[5]F. Pradere and A. Mysyrowicz, in *Proceedings of the Tenth International Conference on the Physics of Semiconductors,* edited by S. P. Keller, J. C. Hensel, and F. Stern (U. S. AEC, Washington, D. C., 1970), p. 101.
[6]R. G. Stafford and M. Sondergeld, Phys. Rev. B 10, 3471 (1974).
[7]T. C. Damen, V. T. Nguyen, and E. Gornik, Solid State Commun. 24, 179 (1977).
[8]V. T. Nguyen, T. C. Damen, E. Gornik, and C. K. N. Patel, Appl. Phys. Lett. 31, 603 (1977).
[9]D. M. Larsen, J. Phys. Chem. Solids 29, 271 (1968).
[10]B. Segall and D. T. F. Marple, in *Physics and Chemistry of II-VI Compounds,* edited by M. Aven and J. J. Prener (North-Holland, Amsterdam, 1967), Chap. 7.
[11]K. J. Button, B. Lax, M. Weiler, and M. Reine, Phys. Rev. Lett. 17, 1005 (1966).
[12]D. G. Seiler, M. W. Goodwin, and M. H. Weiler, Phys. Rev. B 23, 6806 (1981).
[13]Y. S. Park and D. W. Langer, Phys. Rev. Lett. 13, 392 (1964).
[14]Y. S. Park and D. C. Reynolds, Phys. Rev. 132, 2450 (1963).
[15]R. L. Byer, Electro-Opt. Syst. Des. 12, 24 (1980).
[16]F. Bassani and G. Pastori Parravicini, *Electronic States and Optical Transitions in Solids* (Pergamon, New York, 1975), p. 189.
[17]R. A. Faulkner, Phys. Rev. 184, 713 (1969).
[18]D. M. Larsen, private communication. These wave functions are analogous to the 2*S* trial functions described in G. E. Stillman, D. M. Larsen, and C. M. Wolfe, Phys. Rev. Lett. 27, 989 (1971).
[19]H. C. Praddaude, Phys. Rev. A 6, 1321 (1972).
[20]M. Göppert-Mayer, Ann. Phys. (Leipzig) 9, 273 (1931).
[21]F. Bassani and G. Pastori Parravicini, *Electronic States and Optical Transitions in Solids* (Pergamon, New York, 1975), p. 165.
[22]J. H. Bechtel and W. L. Smith, Phys. Rev. B 8, 3515 (1976).
[23]M. Inoue and Y. Toyozawa, J. Phys. Soc. Jpn. 20, 363 (1965).
[24]T. R. Bader and A. Gold, Phys. Rev. 171, 997 (1968).
[25]B. Lax and S. Zwerdling, Prog. Semicond. 15, 221 (1960).
[26]R. L. Aggarwal, Semicond. Semimet. 9, 151 (1972).
[27]H. Venghaus, S. Suga, and K. Cho, Phys. Rev. B 16, 4419 (1977).
[28]E. S. Koteles, in *Excitons,* edited by E. I. Rashba and M. D. Sturge (North-Holland, Amsterdam, 1982).
[29]C. H. Henry and K. Nassau, Phys. Rev. B 2, 997 (1970).
[30]C. Benoit à la Guillaume, J.-M. Debever, and F. Salvan, Phys. Rev. 177, 567 (1969).
[31]D. G. Thomas and J. J. Hopfield, Phys. Rev. 116, 573 (1959).